Numerical Study of the Interacting Bosonic SSH Model

Pietro Scapolo
s337988; pietro.scapolo@studenti.polito.it
Quantum Theory of Condensed Matter
Politecnico di Torino

June 24, 2025

Introduction

We study the interacting bosonic Su-Schrieffer-Heeger (SSH) chain, a one-dimensional lattice model with alternating hopping amplitudes and on-site repulsive interaction. The system is described by the Hamiltonian:

$$H = -\sum_i \left[J + (-1)^i \delta J\right] \left(b_i^\dagger b_{i+1} + \text{h.c.}\right) + \\ + \frac{U}{2} \sum_i n_i(n_i - 1), \tag{1}$$

where $b_i^\dagger$, b_i are bosonic creation and annihilation operators, $n_i = b_i^\dagger b_i$ is the particle number operator, J is the hopping amplitude, δJ introduces dimerization, and U is the on-site interaction strength.

The goal is to analyze how boundary conditions and particle number affect the symmetry of the ground state energy, to compute the charge gap in the thermodynamic limit, and to investigate how the local density distribution changes in different parameter regimes. All simulations are performed at half-filling using QuSpin.

a) Realization of the Hamiltonian

The bosonic SSH Hamiltonian can be implemented in an atomic quantum simulator using ultracold atoms trapped in an optical lattice. The full control over system parameters such as tunneling amplitude, interaction strength and lattice geometry makes these platforms suitable for simulating correlated lattice models [1].

i. Preparation of ultracold atoms.

The first step is to prepare a gas of neutral atoms (e.g., ^{87}Rb or ^{23}Na) at temperatures close to absolute zero. This is achieved using Doppler laser cooling: laser beams are tuned slightly below the atomic transition frequency so that atoms moving toward the beam absorb photons and are slowed down due to momentum transfer. After spontaneous emission, which occurs in random directions, the atom's net velocity is reduced. This process, applied in all spatial directions, cools the gas. Further cooling is obtained via evaporative cooling in a magnetic or optical trap, leading to a Bose-Einstein condensate with high phase coherence [1].

ii. Creation of the optical lattice.

The atoms are trapped in a one-dimensional optical lattice created by two counter-propagating laser beams. Their interference generates a standing wave that produces a periodic potential of the form $V(x) = V_0 \cos^2(kx)$, where $k = 2\pi/\lambda$ and λ is the laser wavelength. The resulting lattice has spacing $a = \lambda/2$, and atoms are localized in the minima of the potential.

To implement the alternating tunneling amplitudes of the SSH model, a second optical lattice is added with double the wavelength of the first one. This creates a superlattice structure in which the depth of the potential alternates from site to site. As a result, the barrier between some pairs of sites is higher than others, reducing the tunneling amplitude selectively. The effective hopping becomes staggered as $J \pm \delta J$, reproducing the dimerization in the Hamiltonian [2].

iii. Control of tunneling amplitudes

The hopping amplitude between neighboring sites depends on the depth of the optical potential. A shallow lattice permits higher tunneling rates, while a deep lattice suppresses tunneling. By adjusting the intensity of the primary and secondary laser fields, one can tune the dimerization parameter δJ, introducing the desired alternation in the hopping terms.

iv. Implementation of on-site interaction

The on-site repulsion U arises from s-wave scattering between bosonic atoms occupying the same site. Its strength can be tuned using magnetic Feshbach resonances. In the strongly interacting regime $U \gg J$, the system approaches the hard-core boson limit, where double occupancy is effectively suppressed.

v. Alternative: Rydberg-based hard-core bosons

A complementary approach uses Rydberg atoms individually trapped in optical tweezers. Atoms are initially in a ground state $|0\rangle$, and excitations to a Rydberg state represent bosonic particles via $b_i^\dagger|0\rangle$. Due to the Rydberg blockade, only one excitation per site is allowed, naturally implementing the hard-core constraint. Dipolar interactions between Rydberg states enable effective hopping between neighboring sites [2, 3].

These experimental techniques allow full control over the parameters J, δJ, and U, making it possible to realize the bosonic SSH Hamiltonian in atomic quantum simulators with high precision. The resulting model corresponds to the target Hamiltonian introduced in Eq. (1).

b) Ground-state symmetry

At fixed filling $N/L = 0.5$, we analyze whether the ground-state energy E_{gs} is symmetric under the inversion $\delta J \mapsto -\delta J$. This property depends on the combination of boundary conditions and system size. Symmetry is expected when the dimerized hopping pattern respects inversion symmetry. Conversely, if the geometry or boundary conditions frustrate this pattern, the symmetry is broken.

i. OBC, even L.

With open boundary conditions and even system size ($L = 6$), the chain has no site or bond exactly at the center, and the dimerization pattern is not symmetric. As a result, reversing δJ produces a physically distinct system, and the ground-state energy is not symmetric.

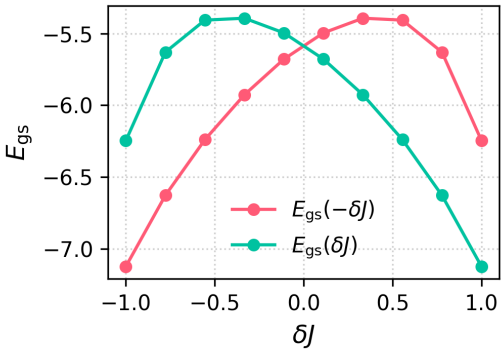

Figure 1: Ground-state energy vs δJ for OBC with $L = 6$, $N = 3$.

ii. OBC, odd L.

For odd $L = 5$, the chain has a central site, and the bond alternation is symmetric with respect to it. The system is invariant under inversion, so E_{gs} is an even function of δJ.

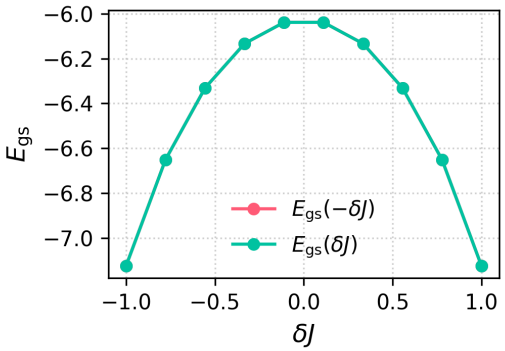

Figure 2: Ground-state energy vs δJ for OBC with $L = 5$, $N = 3$.

iii. PBC, even L.

With periodic boundary conditions and even $L = 6$, the alternation in hopping amplitudes closes perfectly around the ring. The pattern is invariant under translation and inversion, and E_{gs} is symmetric.

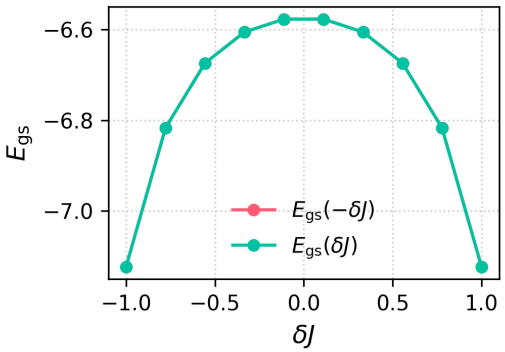

Figure 3: Ground-state energy vs δJ for PBC with $L = 6$, $N = 3$.

iv. PBC, odd L.
For odd $L = 7$, the bond alternation cannot match up periodically. The mismatch introduces frustration in the dimerization pattern, breaking inversion symmetry. This leads to an asymmetric ground-state energy profile.

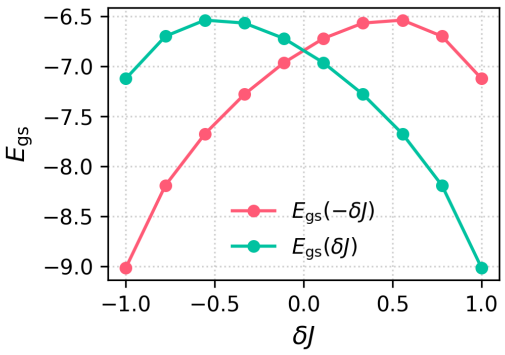

Figure 4: Ground-state energy vs δJ for PBC with $L = 7$, $N = 4$.

c) Charge Gap

We now analyze the behavior of the charge gap, a key quantity for characterizing insulating phases. The charge gap is defined as

$$\Delta_c(L) = E_{\text{gs}}(N+1, L) + E_{\text{gs}}(N-1, L) - 2E_{\text{gs}}(N, L), \tag{2}$$

where $E_{\text{gs}}(N, L)$ denotes the ground state energy of a chain with N bosons on L sites. All simulations are performed at half filling, i.e., $N = L/2$.

i. Finite-size scaling.

For a fixed interaction strength U, we compute $\Delta_c(L)$ for different system sizes L and extrapolate the value in the thermodynamic limit $L \to \infty$. This is achieved by fitting the data as a function of $1/L$ with a quadratic polynomial. Results are shown in Fig. 5 and Fig. 6 for $\delta J = 0.2$ and $\delta J = 0.6$, respectively.

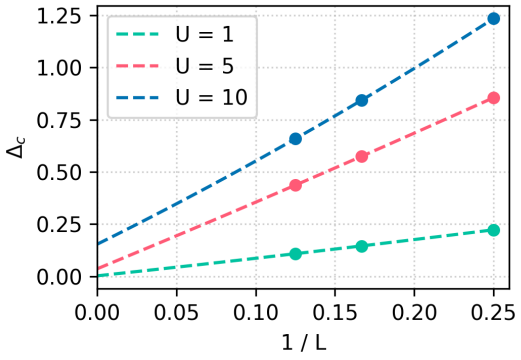

Figure 5: Finite-size scaling of the charge gap Δ_c for different values of U at $\delta J = 0.2$. The lines are polynomial fits in $1/L$.

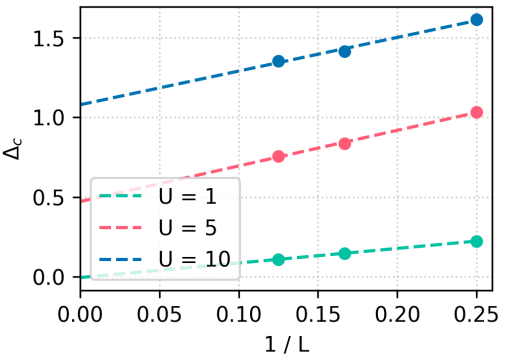

Figure 6: Finite-size scaling of the charge gap Δ_c for different values of U at $\delta J = 0.6$.

ii. Thermodynamic extrapolation.

From the extrapolated fits, we extract the values of $\Delta_c(L \to \infty)$ and plot them as a function of U. The results are presented in Fig. 7 for $\delta J = 0.2$ and in Fig. 8 for $\delta J = 0.6$.

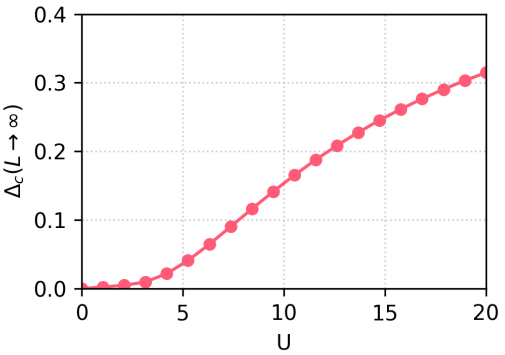

Figure 7: Extrapolated charge gap $\Delta_c(L \to \infty)$ as a function of U for $\delta J = 0.2$.

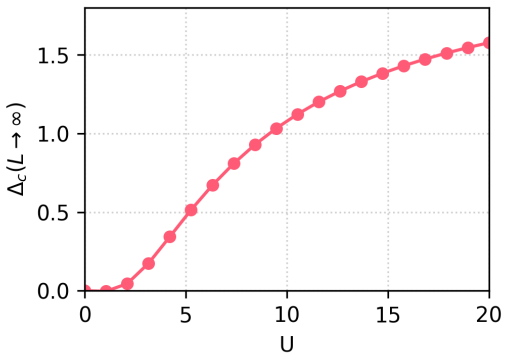

Figure 8: Extrapolated charge gap $\Delta_c(L \to \infty)$ for $\delta J = 0.6$.

d) Local Density Profile

To probe the presence of topological edge states, we analyze the local boson density $\langle n_i \rangle$ under open boundary conditions and a slightly doped filling $N = L/2 + 1$, as suggested in the literature [2]. In this regime, the system exhibits different density profiles depending on the values of δJ and U.

i. Topological phase: $\delta J = -0.7$, $U = 30$
In the strongly interacting regime and for negative dimerization, the bosons accumulate at the edges of the chain. This behavior, illustrated in Fig. 9, is reminiscent of the edge localization observed in the fermionic SSH model and is considered a signature of topological order.

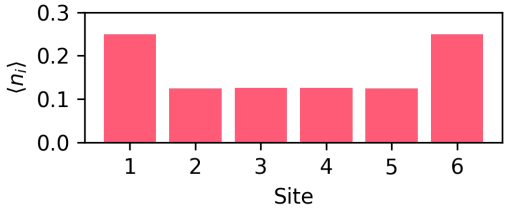

Figure 9: Normalized local density $\langle n_i \rangle / N$ for $\delta J = -0.7$ and $U = 30$. Clear edge accumulation is visible.

ii. Trivial phase: $\delta J = -0.7$, $U = 2$
In the weakly interacting regime, bosons tend to occupy the central sites, leading to a bell-shaped distribution, as shown in Fig. 10. The absence of edge states indicates a trivial insulating phase.

In both cases, the charge gap decreases as U is reduced. For $\delta J = 0.2$, the system becomes gapless around $U \approx 2.5$, with $\Delta_c < 0.1$ already at $U = 5$. In contrast, for $\delta J = 0.6$, the gap closes more slowly and remains finite up to higher values of U. These results suggest a crossover from an insulating to a superfluid-like regime depending on the interaction strength and dimerization.

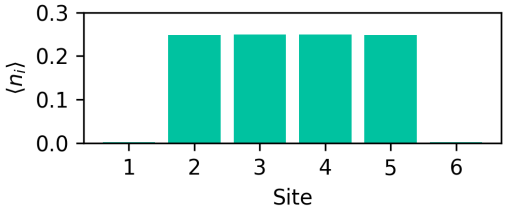

Figure 10: Normalized local density $\langle n_i \rangle / N$ for $\delta J = -0.7$ and $U = 2$. Bosons concentrate in the bulk.

iii. Uniform phase: $\delta J = +0.7$, $U = 30$
For large repulsion but positive dimerization, the bosons are homogeneously distributed along the chain. As seen in Fig. 11, this regime lacks both bulk and edge localization.

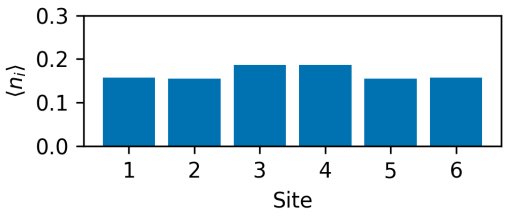

Figure 11: Normalized local density $\langle n_i \rangle / N$ for $\delta J = +0.7$ and $U = 30$. The distribution is nearly flat.

These results suggest that topological edge states emerge only for negative δJ and sufficiently strong on-site interaction. The variation in local density profiles reflects the different phases and allows a visual characterization of the system's topology.

References

[1] D. Jaksch and P. Zoller, *The cold atom Hubbard toolbox*, Annals of Physics **315**, 52–79 (2005).

[2] F. Grusdt, M. Hoening, and M. Fleischhauer, *Topological edge states in the one-dimensional superlattice Bose-Hubbard model*, Phys. Rev. Lett. **110**, 260405 (2013).

[3] H. Labuhn *et al.*, *Tunable two-dimensional arrays of single Rydberg atoms for realizing quantum Ising models*, Nature **534**, 667–670 (2016).